Cancer Cell International

RESEARCH

Open Access

Hsa_circ_0072088 promotes non-small cell lung cancer progression through modulating miR-1270/TOP2A axis

Sixuan Li[1,2], Zhigang Cui[4], Min Gao[2], Yanan Shan[2], Yihong Ren[2], Yuxin Zhao[2], Di Wang[2], Tingyu Meng[2], Hongxu Liu[3*] and Zhihua Yin[2*]

Abstract

According to the data released by the International Agency for Research on Cancer (IARC) in 2020, lung cancer ranks second among newly diagnosed malignant tumors globally. As a special class of non-coding RNA, circRNA has become a new hotspot in the field of biomarker research. With the continuous deepening of molecular—level investigations, the underlying mechanisms of circRNA are being gradually unveiled. The more widely studied mechanism is the competitive endogenous RNA mechanism of circRNA. Studies related to circRNA expression were searched in GEO database and statistically analyzed using the "limma" package and weighted gene co-expression network analysis. The expression of circRNA, microRNA and mRNA in cells and tissues were examined via qRT-PCR. MTS assay was used to measure cell proliferation, Transwell assay was used to measure cell migration, and apoptosis assay was carried out to detect cell apoptosis. Additionally, a dual—luciferase reporter assay was further executed to explore the targeted binding relationships between circRNA-microRNA and microRNA-mRNA. It was discovered that hsa_circRNA_103809 was differentially highly expressed in non—small cell lung cancer cells, whereas miR—1270 was differentially lowly expressed. The knockdown of circ_0072088 inhibited the cell proliferation and migration, while promoting cell apoptosis. The same biological function was found with the overexpression of miR-1270. The rescue experiment further validated that circ_0072088 could regulate the biological function of cells by influencing miR-1270. Finally, the targeted binding relationship was verified by dual luciferase reporting experiment. In conclusion, circ_0072088 is differentially highly expressed in non-small cell lung cancer and can affect the progression of non-small cell lung cancer through the circ_0072088/miR-1270/TOP2A axis.

Keywords Non-small cell lung cancer, Circ_0072088, MiR-1270, TOP2A gene, Competitive endogenous RNA mechanism

*Correspondence:
Hongxu Liu
hxliu@cmu.edu.cn
Zhihua Yin
zhyin@cmu.edu.cn
Full list of author information is available at the end of the article

Introduction

According to the GLOBOCAN 2020 data released by the International Agency for Research on Cancer (IARC), there were 2.2 million newly diagnosed lung cancer cases globally in 2018, accounting for 11.4% of all new cancer cases. The number of deaths due to lung cancer reached 1.8 million, accounting for 18.0% of all cancer—related deaths. Lung cancer ranks second in cancer incidence and first in mortality worldwide [1]. By integrating the cancer incidence and mortality estimates from GLOBOCAN 2020 data with China's cancer statistics in 2015, it was found that lung cancer remains the most prevalent cancer in China. In 2020, approximately 820,000 new lung cancer cases were reported in China, and about 720,000 deaths were attributed to lung cancer, making it the leading cause of cancer—related death [2]. Since late—stage diagnosis affects the treatment and prognosis of lung cancer, the exploration of potential biomarkers and therapeutic targets for lung cancer has become the focus of current research.

Circular RNA (circRNA), a special type of non-coding RNA, has a closed ring structure and is formed by the reverse splicing of downstream splicing donors and upstream splicing receptors [3]. In 1976, Sanger et al. proposed that viroids were covalently closed circular RNA molecules [4]. In 1979, Hsu et al. observed the circular form of RNA in the cytoplasm of HeLa cells [5]. CircRNAs were originally thought to have originated from viruses, but with further study, researchers found that circRNAs can be produced by transcription of endogenous genes. In 1991, researchers discovered new splicing products through the study of DCC (deleted in colon cancer) gene, which showed that the presence of disturbing transcription factors interfered with the splicing process and produced new RNA products [6]. In 1993, Cocquerelle et al. found that mis-splicing produced circular RNA molecules, and their research suggested that the mechanism of mis-splicing was mainly an intramolecular process [7]. In the same year, studies by Capel et al. indicated that the circular transcript originated from a normal splicing process due to the abnormal genomic structure around the mouse Sry gene [8]. As scientific research progresses, an increasing number of circRNAs have been discovered, and an ever growing array of their functions have also come to light.

Because of its special covalent closed structure, circular RNA is not easily degraded by RNase and exhibits higher stability [9]. The main biological functions of circRNA include serving as competing endogenous RNA (ceRNA). Specifically, circRNA can bind to microRNA through microRNA response elements (MREs), subsequently influencing the expression of downstream mRNA targeted by the microRNA [10, 11]. The ceRNA mechanism of circular RNA has been demonstrated in a variety of tumors, and the ceRNA mechanism of circular RNA plays an important role in tumor development and drug resistance of cancer patients during treatment. In the study of gastric cancer, circNRIP1 regulates the expression of miR-149-5p by acting as an endogenous microRNA "sponge" of miR-149-5p. This, in turn, affects the expression of its downstream gene AKT1, and ultimately impacts the AKT1/mTOR signaling pathway, thus influencing the progression of gastric cancer [12]. Luo et al.'s study found that circCCDC9 regulates CAV1 by influencing the expression of miR-6792-3p, thus affecting the progression of gastric cancer [13]. Peng et al. found that the circCUL2/miR-142-3p/ROCK2 axis may be a key mechanism in gastric cancer [14]. In breast cancer-related studies, circMMP11 affects breast cancer progression via the circMMP11/miR-625-5p/ZEB2 axis [15]. Research by Xu et al. found that circTADA2As plays a role in breast cancer by targeting the miR-203a-3p/SOCS3 axis [16]. In studies related to bladder cancer, circSLC8A1 can exert its effect in bladder cancer by targeting miR-130b/miR-494 to regulate PTEN [17]. In the study related to cervical cancer, Zhang et al. found that hsa_circ_0043280 regulates the growth and metastasis of cervical cancer through the miR-203a-3p/PAQR3 axis [18]. In lung cancer-related studies, hsa_circRNA_0017620 has been found to regulate the progression of non-small cell lung cancer through the miR-520a-5p/KRT5 axis [19]. Ma et al. found that circMAN2B2 affects the biological function of lung cancer cells through the miR-1275/FOXK1 axis [20]. Studies has found that circTAB2 affects the proliferation, migration and invasion of lung cancer cells by acting as a miR-3142 "sponge" and regulating GLIS2 expression [21]. In conclusion, through the ceRNA mechanism, circRNA significantly impacts tumor development and drug resistance during cancer treatment.

Method

Research sample

In this study, the lung cancer tissue samples associated with circRNA expression were retrieved from the Gene Expression Omnibus (GEO) public database, while the lung cancer tissue samples related to mRNA expression were obtained from The Cancer Genome Atlas (TCGA) public database.

The 29 cases of lung cancer in this study were from lung cancer patients admitted to Shengjing Hospital affiliated to China Medical University from January 2020 to December 2020. Informed consent of the lung cancer patients has been obtained and this study was approved by the Medical Ethics Committee of China Medical University. The inclusion criteria of the subjects were: (1) Confirmed pathological diagnosis of lung cancer; (2) No

radiotherapy or chemotherapy was performed before sample collection.

Screening of differentially expressed genes in lung cancer

In GEO data analysis, the three data sets were integrated first, and the 'ComBat' package of R software was used to correct the data in batches. R software was used to standardize the data in TCGA database. The 'limma' package of R software was used to screen differentially expressed circRNAs and mRNAs in lung cancer and para-cancer tissues. CircRNAs differentially expressed in lung cancer tissues and adjacent tissues were analyzed in GEO database, and the fold change was set to 1.5, and the P-value (padj) was set to 0.05. The different-expressed mRNAs in lung cancer tissues were analyzed by TCGA database, and the fold change was set to 2, and the P-value (padj) was set to 0.01. The differentially expressed circRNAs and mRNAs in lung cancer tissues were visualized by drawing volcano plots and heat maps.

Constructing the weighted gene co-expression network

Sample pretreatment and determination of soft threshold β

First, check whether the sample contains missing values, and further conduct cluster analysis on the sample to detect whether the sample contains abnormal outliers. In addition, sample clustering is combined with clinical characteristics. By using the pickSoftThreshold function of R software, the scale-free network was constructed according to the expression matrix, and the optimal β value was determined by the scale-free network fitting index $R^2$and the average connectivity of genes.

Constructing topological overlapping matrix

Firstly, the correlation matrix between genes was constructed, and Pearson correlation coefficient was used to calculate the correlation between two genes. And take the absolute value of the correlation coefficient (value range: 0–1), the formula is as follows:

$$s_{ij} = \left|cor(i,j)\right| \tag{1}$$

where i and j represent i gene and j gene respectively.

Furthermore, the soft threshold β was combined to convert the correlation matrix to the adjacency matrix. The calculation formula is:

$$a_{ij} = \left|cor(i,j)\right|^{\beta} \tag{2}$$

Adjacency matrix mainly considers the relationship between two genes, while Topological overlap matrix (TOM) not only discusses the correlation between two genes, but also considers the intermediate node genes. The calculation formula is:

$$\omega_{ij} = \frac{l_{ij} + a_{ij}}{\min\left\{k_i, k_j\right\} + 1 - a_{ij}} \tag{3}$$

$$l_{ij} = \sum_{u} a_{iu} a_{uj} \tag{4}$$

$$k_i = \sum_{u} a_{iu} \tag{5}$$

where u represents the node gene that is co-related with the i gene and the j gene.

In order to further divide modules, it is necessary to obtain the $disTOM_{ij}$, and the calculation formula is as follows:

$$disTOM_{ij} = 1 - \omega_{ij} \tag{6}$$

Constructing gene modules

Topological overlap matrix (TOM) was converted into Dissimilarity matrix, and hierarchical clustering tree was constructed by hclust function based on the differences between genes. The genes with high topological overlap in the clustering tree can be gathered together, and the gene modules were divided by dynamic tree cut method, and different colors were used to mark the modules. Module eigengenes were obtained by principal component analysis of all genes in the module, which can represent the overall gene expression level of the module. Furthermore, cluster analysis was carried out to combine the modules with high module similarity.

Association between gene modules and clinical information

The clinical information included in this study was sample type (cancerous tissue/para-cancerous tissue) and patient gender. Firstly, modules related to clinical features were determined according to the correlation between module eigenvalues and clinical features. The correlation coefficient between each gene and different clinical features was further calculated to obtain Gene Significance (GS). Module Membership (MM) was obtained by calculating the correlation between genes and module eigenvalues. The scatter-plot of genes within the module was further drawn, and the genes with high MM and GS (the genes in the upper right corner of the scatter-plot) were selected as the key genes.

Online forecasting database

This research through the use of the online database to predict the interaction between genes, using starbase (ENCORI) database (https://starbase.sysu.edu.cn/) explore the interaction between circRNA and

microRNA. Using starbase (ENCORI) database (https://starbase.sysu.edu.cn/), miRWalk database (http://mirwalk.umm.uni-heidelberg.de/) and TargetScan database (http://www.targetscan.org/) to investigate the interaction between microRNA and mRNA.

Cell culture

The cell lines involved in this study are non-small cell lung cancer cell lines: A549 cell line and SK-MES-1 cell line, as well as normal lung epithelial cell line BEAS-2B. All cell lines were provided by Shanghai Genechem Co., Ltd., (Shanghai, China). The A549 cell line was cultured with F12K complete culture medium, SK-MES-1 cell line was cultured with MEM complete culture medium, and BEAS-2B cell line was cultured with DMEM complete culture medium. The operation was carried out under strict aseptic conditions and cultured in a constant temperature and humidity incubator (37 °C, 5%CO_2).

Cell extraction and quantitative real time-polymerase chain reaction (qRT-PCR)

Total RNA was extracted from cells and tissues using RNAiso Plus (TaKaRa, Tokyo, Japan) reagent. CircRNA and mRNA was reverse transcribed into cDNA using PrimeScript™ RT reagent Kit with gDNA Eraser (TaKaRa, Tokyo, Japan) reagent, while microRNA using Mir-X miRNA First-Strand Synthesis Kit (TaKaRa, Tokyo, Japan) reagent. The polymerase chain reaction was further performed with TB Green® Premix Ex Taq™ II (TaKaRa, Tokyo, Japan) reagent. The primer sequences of miR-1270, internal reference U6 and GAPDH were provided by RiboBio (Guangzhou, China). The primer sequences of circ_0072088 and TOP2A were shown in Table S1.

Cell transfection

In this study, the overexpressed plasmid of circ_0072088 and its corresponding control plasmid vector were constructed by SyngenTech Co. Ltd. (Beijing, China). Small interference RNA (siRNA) targeting circ_0072088 and the corresponding NC were also obtained from SyngenTech Co. Ltd. (Beijing, China). The miR-1270 mimics and relative NC were obtained from RiboBio (Guangzhou, China). Jetprime reagent was used for cell transfection.

Cell proliferation assay

Prepare a cell suspension and transfer it to a 15 mL centrifuge tube. Dilute the cell suspension to a concentration of $2–2.5\times10^4$ cells/mL and mix thoroughly. For the cell proliferation assay in 96-well cell culture plates, add 100 μL of the diluted cell suspension to each well, with five replicate wells per group. To exclude the influence of the culture medium on absorbance, add only culture medium to some wells. Place the plate in the incubator. Set the detection time points at 0 h, 24 h, 48 h, and 72 h. Before detection, add 20 μL of MTS (Promega, USA) working solution to each well, mix well, and incubate in the incubator for 2 h. Finally, measure the absorbance at 490 nm.

Cell migration assay

Starve the cells for 24 h using serum-free incomplete culture medium. After 24 h, prepare the cell suspension and transfer it to a 15 mL centrifuge tube, diluting it to a concentration of $1.5–2\times10^5$ cells/mL. Add 500 μL of complete culture medium to the lower chamber of the Transwell insert, and add 200 μL of the cell suspension to the upper chamber of the Transwell insert, avoiding the formation of bubbles. Place the Transwell insert into the cell culture incubator. After 24 h, fix the cells with methanol, and then stain with crystal violet. Observe the stained cells using a microscope (Echo, USA) and take photos of five fields of view.

Cell apoptosis assay

Prepare a cell suspension and transfer it to a 15 mL centrifuge tube. After centrifugation, discard the culture medium, resuspend the cell pellet in PBS by pipetting, and centrifuge again. Discard the PBS and keep the cells on ice for further use. Resuspend the cell pellet in the Binding Buffer from the apoptosis detection kit (KeyGen Biotech, China) by pipetting to form a cell suspension. Divide the cells into several groups for detection: Control cells (unstained), cells stained with V-APC only, cells stained with 7-AAD only, cells stained with both V-APC and 7-AAD as a control group, and cells stained with both V-APC and 7-AAD as the experimental group. Incubate the cells in the dark for 15 min, then analyze the level of apoptosis using a flow cytometer (Millipore, USA).

Dual-luciferase reporter assay

Transfect cells in a 24-well cell culture plate. After 48 h of transfection, discard the culture medium. Add Passive Lysis Buffer (Promega, USA) to each well to lyse the cells. Incubate in the dark on a horizontal shaker for 15 min. Transfer the cell lysate to a centrifuge tube and centrifuge. Collect the supernatant into a new centrifuge tube.

In a microplate, add 10 μL of PLB lysate to each well, followed by 100 μL of LAR II (Luciferase Assay Substrate). Measure the firefly luciferase signal using a multifunctional microplate reader. Add 100 μL of Stop & Glo® Reagent to each well. Measure the Renilla luciferase signal using a multi-functional microplate reader. Set up three replicate wells per group.

Statistical analysis

In this study, we performed three replicate experiments to ensure the reliability of the results, and $P<0.05$ was considered statistically significant. The T test is used to detect the difference between two groups of samples.

Results

Differential expression of circRNAs in lung cancer screening based on the 'limma' package

The three datasets GSE101586, GSE101684 and GSE112214 were integrated, and the differentially expressed circRNAs in lung cancer tissues and adjacent normal tissues were obtained by using the 'limma' package of R software. In this part of study, the fold change was set to 1.5 and the padj was set to 0.05. After difference analysis, it was found that hsa_circRNA_103809 (hsa_circ_0072088) was differentially highly expressed in lung cancer tissues compared with adjacent normal tissues. Hsa_circRNA_102442 (hsa_circ_0049271), hsa_circRNA_102046 (hsa_circ_0043256), hsa_circRNA_103415 (hsa_circ_0008234) and hsa_circRNA_103820 (hsa_circ_0072309) were differentially lowly expressed in lung cancer tissues. In order to visualize the results of differential analysis, volcano plot and heat map of differentially expressed circRNAs were drawn, as shown in Fig. 1.

Differentially expressed circRNAs screening in lung cancer based on WGCNA

First, it was determined that there were no missing values in the samples, and further hierarchical clustering analysis found that there were no outlier samples in this study, as shown in Fig. 1C, D. In order to make the constructed gene co-expression network conform to scale-free network, it is necessary to determine the optimal soft threshold β, and further convert the correlation matrix between genes into an adjacency matrix. In this study, the scale-free network fitting index R^2 was set at 0.8, and the optimal soft threshold β was 12, as shown in Fig. 1E, F.

Then it was further transformed into a topological matrix. Based on the calculated dissimilarity, a hierarchical clustering tree was generated. The 'cutreeDynamic' function of R software was used to divide the modules. A total of 32 modules were obtained, with each module assigned a distinct color (minModuleSize = 30). By conducting hierarchical clustering analysis on the calculated module eigengenes of each module, the modules with high similarity were merged, and 17 modules were finally obtained, as shown in Fig. 1G. The correlation between module eigengenes and clinical features was analyzed, and heat plot is shown in Fig. 1H. In the figure, darkturquoise module and darkorange module are highly correlated with the sample type.

Module Membership (MM) was obtained by calculating the correlation between genes and module eigengenes. As shown in Fig. 2A, B, Gene Significance (GS) was set as the Y axis, Module Membership (MM) was set as the X axis. Threshold values of GS > 0.65 and MM > 0.85 were set. Key genes in darkturquoise module and darkorange module, along with their related GS and MM values, are shown in Table S2 and Table S3 respectively. As shown in Fig. 2C, hsa_circRNA_103809 (hsa_circ_0072088) was obtained by the intersection of 5 differentially expressed circRNAs analyzed by the 'limma' package of R software and 12 circRNAs analyzed by WGCNA.

Differentially expressed mRNAs in lung adenocarcinoma and lung squamous cell carcinoma based on TCGA database

The gdc-client download tool was used to download the data. The TCGA-LUAD samples included 496 cancer tissue samples and 55 para-cancer tissue samples. The TCGA-LUSC samples included 502 cancer tissue samples and 49 para-cancer tissue samples. R software was used to obtain differentially expressed mRNAs, and the differentially expressed genes were visualized by volcano plot and heat map. In this study, 2,542 differentially expressed mRNAs were obtained in lung adenocarcinoma through differential analysis, among which 2,032 were differentially highly expressed and 510 were differentially lowly expressed. The volcano plot and heat map were shown in Fig. 2D, E. A total of 3778 differentially expressed mRNAs were identified in lung squamous cell carcinoma. Among them, 2650 mRNAs were differentially highly expressed, while 1128 were differentially lowly expressed. The volcano pot and heat map were shown in Fig. 2F, G.

Determination of the ceRNA network

The microRNA interacting with hsa_circRNA_103809 (hsa_circ_0072088) was investigated through starbase

(See figure on next page.)

Fig. 1 Volcano plot and heat map of differentially expressed circRNAs in lung cancer tissues, **A** volcano map **B** heat map, green indicating low expression in cancer tissues while red indicating high expression in cancer tissues; **C** the hierarchical clustering tree of the research samples; **D** the sample hierarchical clustering tree and corresponding clinical characteristics of the sample; **E** relationship between the soft threshold β and the scale-free network fitting index R^2; **F** Relationship between the soft threshold β and the average connectivity; **G** Division and merging of modules; **H** Heat plot of correlation between gene modules and clinical features

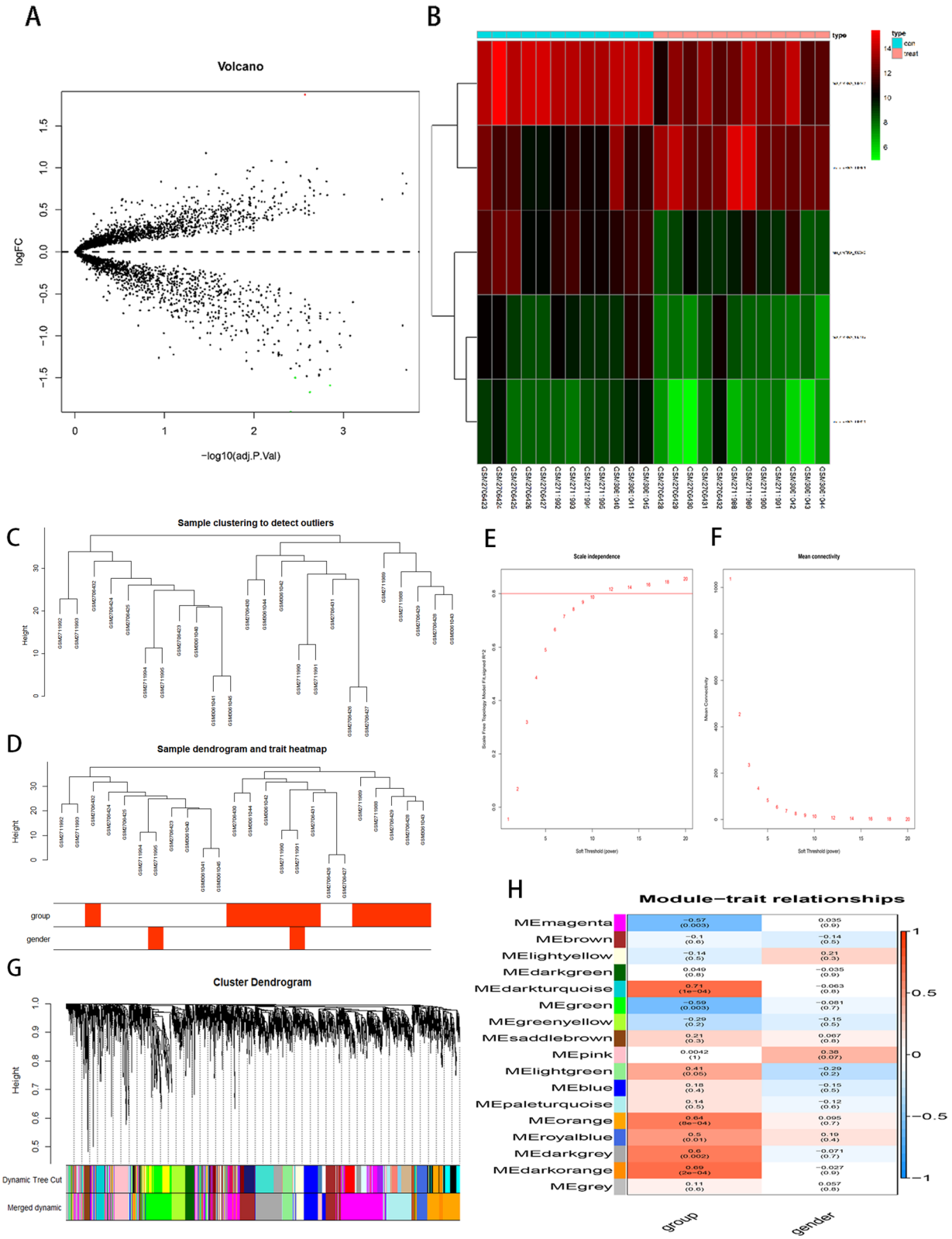

Fig. 1 (See legend on previous page.)

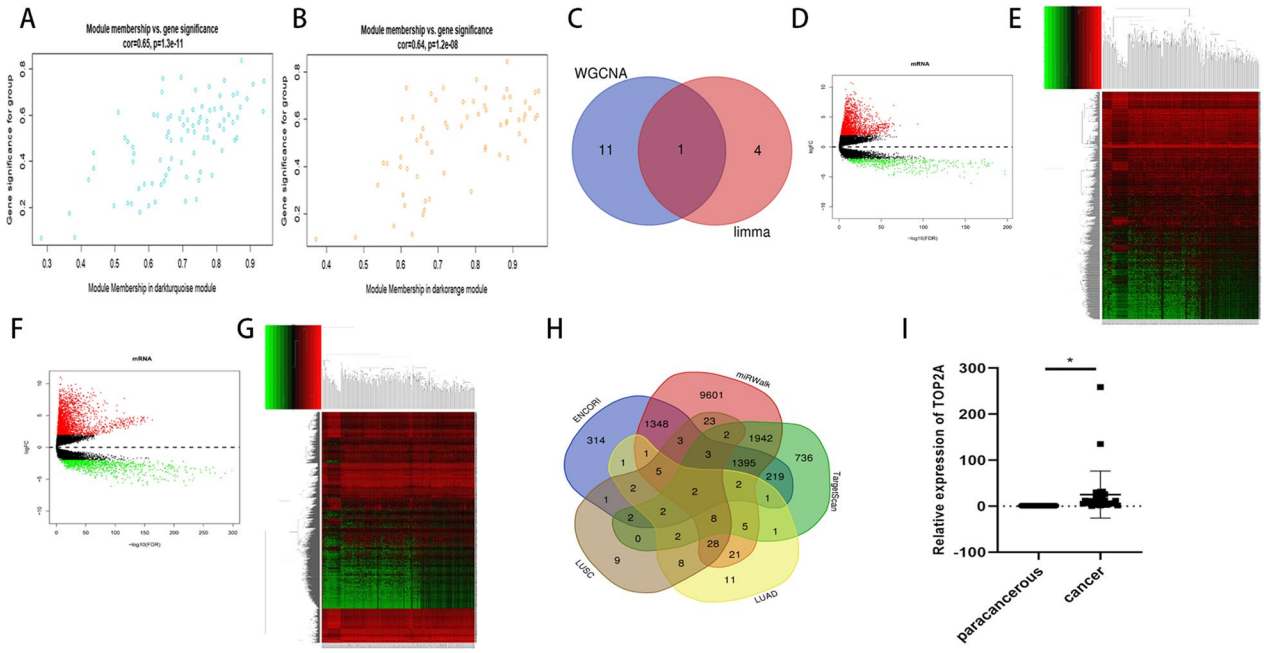

Fig. 2 **A** Scatter plot of genes in the darkturquoise module; **B** Scatter plot of genes in darkturquoise module; **C** Intersection of 5 differentially expressed circRNAs analyzed by the 'limma' package of R software and 12 circRNAs analyzed by WGCNA; **D** the volcanic plot of differentially expressed mRNAs in LUAD; **E** the heat map of differentially expressed mRNAs in LUAD. **F** the volcanic plot differentially expressed mRNAs in LUSC; **G** the heat map of differentially expressed mRNAs in LUSC. Red is high expression and green is low expression; **H** the intersection of the predicted mRNAs and the top 100 mRNAs with differentially high expression in lung adenocarcinoma and lung squamous cell carcinoma analyzed by TCGA database; **I** Expression of TOP2A gene in lung cancer tissue samples

(ENCORI) database. The interaction site was located at hsa_circ_0072088, and miR-1270 was discovered as the interacting microRNA. In this study, the mRNAs interacting with miR-1270 were predicted by starbase (ENCORI) database, miRWalk database and TargetScan database. The intersection of the predicted mRNAs and the top 100 mRNAs with differentially high expression in lung adenocarcinoma and lung squamous cell carcinoma analyzed by TCGA database was taken, as shown in Fig. 2H. As a result of the intersection, two mRNAs, TOP2A and ANLN, were obtained. In this study, TOP2A, which showed more significant difference, was selected as the gene for further investigation. The matching sequences between circRNA and miRNA, miRNA and mRNA are presented in the supplementary figure.

Expression of TOP2A gene in tissue samples

The expression of TOP2A gene in lung cancer was further verified using lung cancer tissue samples. As shown in Fig. 2. I, it was found that TOP2A gene was differentially highly expressed in lung cancer tissues compared with adjacent tissues ($P<0.05$). Based on the median expression level, the samples were further classified into a high—expression group and a low—expression group. Table 1 presents the distribution of the TOP2A high—expression and low—expression groups in relation to different clinical characteristics.

Previous medical history mainly included hypertension, diabetes, coronary heart disease, hepatitis, and tuberculosis.

The relative expression and biological function of circ_0072088 in lung adenocarcinoma and lung squamous cell carcinoma

In this study, the expression of circ_0072088 was detected by qRT-PCR using human normal lung epithelial BEAS-2B cell line, lung adenocarcinoma A549 cell line, and lung squamous cell carcinoma SK-MES-1 cell line. As shown in Fig. 3A, compared with BEAS-2B cell line, circ_0072088 was differentially highly expressed in A549 cell line and SK-MES-1 cell line (A549: $P<0.01$; SK-MES-1: $P<0.01$).

In order to further investigate the biological function of circ_0072088 in lung adenocarcinoma and lung squamous cell carcinoma, we constructed a small interference fragment of siRNA-circ_0072088 to knock down the expression of circ_0072088, and the qRT-PCR results were shown in Fig. 3B, C. After transfection, the expression of circ_0072088 in A549 cells and SK-MES-1 cells

Table 1 The distribution of TOP2A expression in different clinical features in lung cancer tissue samples

Clinical features	Low expression	High expression	*P*
Gender			
Male	7	11	0.264
Female	7	4	
Age			
≤ 60	7	6	0.715
> 60	7	9	
Smoke			
No	7	5	0.462
Yes	7	10	
Drink			
No	8	10	0.710
Yes	6	5	
PAST medical history			
No	9	11	0.700
Yes	5	4	
T			
T1–T2	11	9	0.427
T3–T4	3	6	
N			
N0	8	13	0.109
N1–N2	6	2	

was decreased, and the difference was statistically significant (A549: $P<0.001$; SK-MES-1: $P<0.001$).

In this study, the expression of circ_0072088 in A549 cells and SK-MES-1 cells was knocked down by transfecting siRNA-circ_0072088, and cell proliferation experiment was used to further investigate the regulatory effect of circ_0072088 on cell proliferation of lung adenocarcinoma cells and lung squamous cell carcinoma cells. The results were shown in Fig. 3D, E. Compared with si-NC, circ_0072088 knockdown inhibited cell proliferation of A549 cells and SK-MES-1 cells (A549: $P<0.001$; SK-MES-1: $P<0.01$).

Transwell cell migration assay was used to investigate the effect of circ_0072088 knockdown on cell migration of A549 cells and SK-MES-1 cells. As shown in Fig. 3F, knocking down circ_0072088 inhibited cell migration in A549 cells ($P<0.001$). As shown in Fig. 3G, the cell migration ability of SK-MES-1 cells was also significantly decreased after knocking down circ_0072088 ($P<0.001$).

In order to explore the effect of circ_0072088 on apoptosis of lung adenocarcinoma cells and lung squamous cell carcinoma cells, apoptosis experiments were performed, and the results were shown in Fig. 3H, I. In A549 cells, compared with the si-NC group, the apoptosis of cells transfected with siRNA-circ_0072088 was increased and the difference was statistically significant ($P<0.01$). Similarly, in SK-MES-1 cells, knockdown circ_0072088 had the biological function of promoting apoptosis ($P<0.01$).

The relative expression and biological function of miR-1270 in lung adenocarcinoma and lung squamous cell carcinoma

The expression of miR-1270 in normal lung epithelial BEAS-2B cells, lung adenocarcinoma A549 cells and lung squamous cell carcinoma SK-MES-1 cells was detected by qRT-PCR assay, as shown in Fig. 4A. Compared with BEAS-2B cells, the expression of miR-1270 was significantly lower in A549 cells and SK-MES-1 cells (A549, $P<0.001$; SK-MES-1, $P<0.001$).

The expression of miR-1270 was observed after circ_0072088 knockdown in A549 cells and SK-MES-1 cells. As shown in Fig. 4B, C, compared with the transfected si-NC group, the expression of miR-1270 in the transfected siRNA-circ_0072088 group was significantly increased (A549, $P<0.001$; SK-MES-1, $P<0.01$).

The overexpression model of miR-1270 was further constructed, and its transfection efficiency was detected by qRT-PCR. As shown in Fig. 4D, E, it was found that transfected miR-1270 mimics significantly increased the expression of miR-1270 compared with transfected miR-1270 NC (A549, $P<0.001$; SK-MES-1, $P<0.001$).

As shown in Fig. 4F, G, it was found that in A549 cells, compared with the miR-1270 NC group, the proliferation ability of cells transfected with miR-1270 mimics decreased, and the difference was statistically significant ($P<0.001$). The proliferation ability of SK-MES-1 cells was also decreased after the overexpression of miR-1270 ($P<0.001$).

Transwell cell migration assay was performed to detect the migration ability of cells transfected with miR-1270 mimics and miR-1270 NC. Results As shown in Fig. 4H, I, compared with transfection of miR-1270 NC, A549 cells transfected with miR-1270 mimics significantly reduced cell migration ability ($P<0.001$). It was also found that overexpression of miR-1270 inhibited cell migration in SK-MES-1 cells ($P<0.001$).

The effect of miR-1270 on apoptosis of lung adenocarcinoma cells and lung squamous cell carcinoma cells was investigated through apoptosis experiments, as shown in Fig. 4J, K. In A549 and SK-MES-1 cells, overexpression of miR-1270 promoted apoptosis (A549, $P<0.001$; SK-MES-1, $P<0.05$).

circ_0072088 affects the biological function of lung adenocarcinoma cells and lung squamous cell carcinoma cells by regulating miR-1270

In order to further explore the interaction between circ_0072088 and miR-1270, the circ_0072088

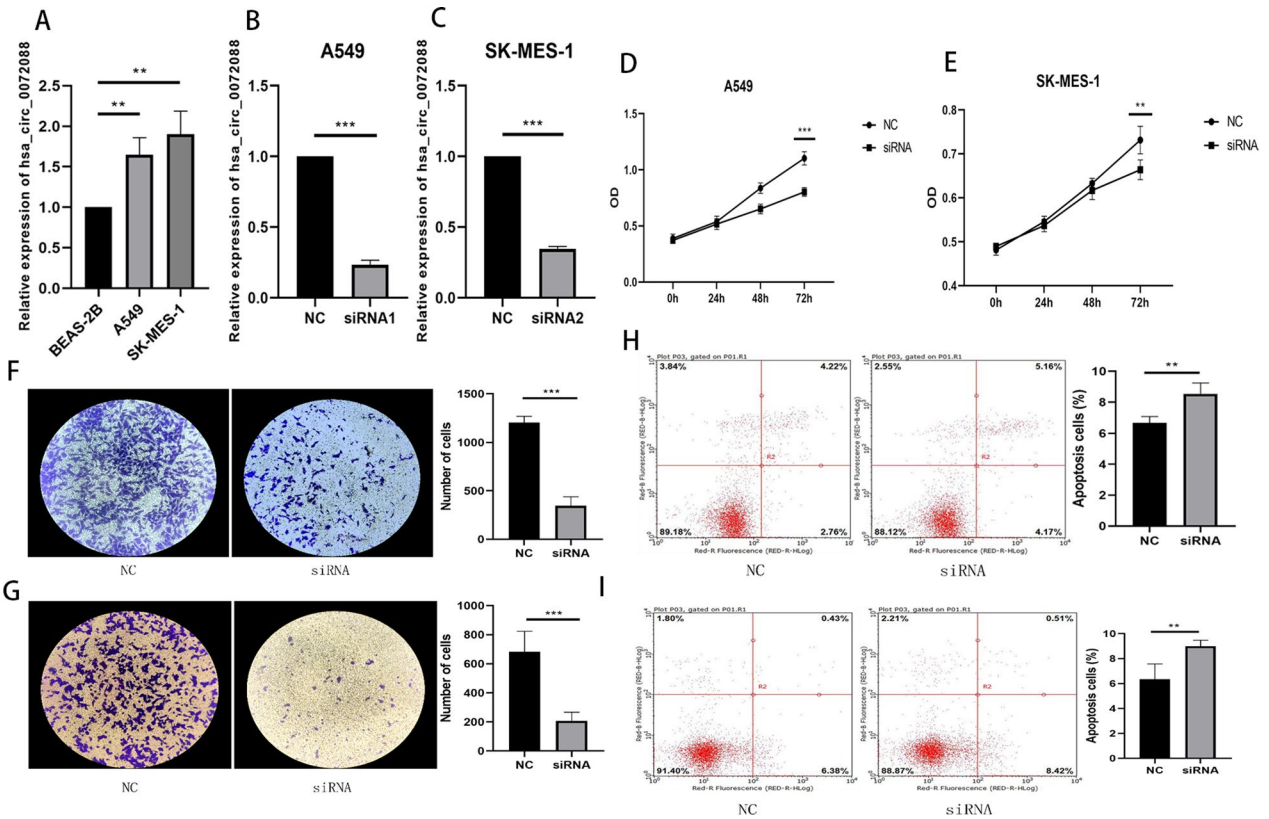

Fig. 3 **A** Expression of circ_0072088 in BEAS-2B cells, A549 cells and SK-MES-1 cells. **B** Expression of circ_0072088 in A549 cells after transfection of si-NC and siRNA-cir_0072088; **C** Expression of circ_0072088 in in SK-MES-1 cells after transfection of si-NC and siRNA-cir_0072088; **D** Knockdown of circ_0072088 inhibited the proliferation of A549 cells; **E** Knockdown of circ_0072088 inhibited the proliferation of SK-MES-1 cells; **F** Knockdown of circ_0072088 inhibited the cell migration of A549 cells; **G** Knockdown of circ_0072088 inhibited the cell migration ability of SK-MES-1 cells; **H** Knockdown of circ_0072088 promoted apoptosis of A549 cells; **I** Knockdown of circ_0072088 promoted apoptosis of SK-MES-1 cells

overexpression plasmid was constructed and transfected to construct the circ_0072088 overexpression model. The qRT-PCR results are shown in Fig. 5A, B, and the differences are statistically significant (A549, $P<0.01$; SK-MES-1, $P<0.001$).

Through the rescue experiment, we verified the interaction between circ_0072088 and miR-1270. The cells were divided into three groups by co-transfection: circ_0072088 NC + miR-1270 NC group, circ_0072088 OE + miR-1270 NC group and circ_0072088 OE + miR-1270 mimics group. As shown in Fig. 5C, D, the proliferation experiment showed that compared with circ_0072088 NC + miR-1270 NC group, the cell proliferation ability of circ_0072088 OE + miR-1270 NC group was increased in A549 cells ($P<0.01$). However, circ_0072088 OE + miR-1270 mimics group could restore the cell proliferation ability which was increased due to circ_0072088 overexpression ($P<0.001$). In SK-MES-1 cells, it was found that the cell proliferation ability was increased after the overexpression of circ_0072088 ($P<0.05$), while the overexpression of miR-1270 could inhibit the increased cell proliferation ability due to the overexpression of circ_0072088 ($P<0.001$).

As shown in Fig. 5E, F, in A549 cells, the overexpression of circ_0072088 promoted cell migration ($P<0.01$), and the overexpression of miR-1270 could restore the promotion of cell migration caused by the overexpression of circ_0072088 ($P<0.001$). Similarly in SK-MES-1 cells, co-transfected circ_0072088 OE + miR-1270 NC group had enhanced cell migration ability compared with circ_0072088 NC + miR-1270 NC group ($P<0.05$). Co-transfection of circ_0072088 OE + miR-1270 mimics group inhibited cell migration enhanced by circ_0072088 overexpression ($P<0.001$).

As shown in Fig. 5G, H, compared with circ_0072088 NC + miR-1270 NC group, the overexpression of circ_0072088 in A549 cells inhibited apoptosis of A549 cells ($P<0.01$). Compared with circ_0072088 OE + miR-1270 NC group, circ_0072088 OE + miR-1270 mimics group promoted cell apoptosis ($P<0.01$). Similarly, the overexpression of circ_0072088 in SK-MES-1 cells inhibited the apoptosis of SK-MES-1 cells ($P<0.05$), and

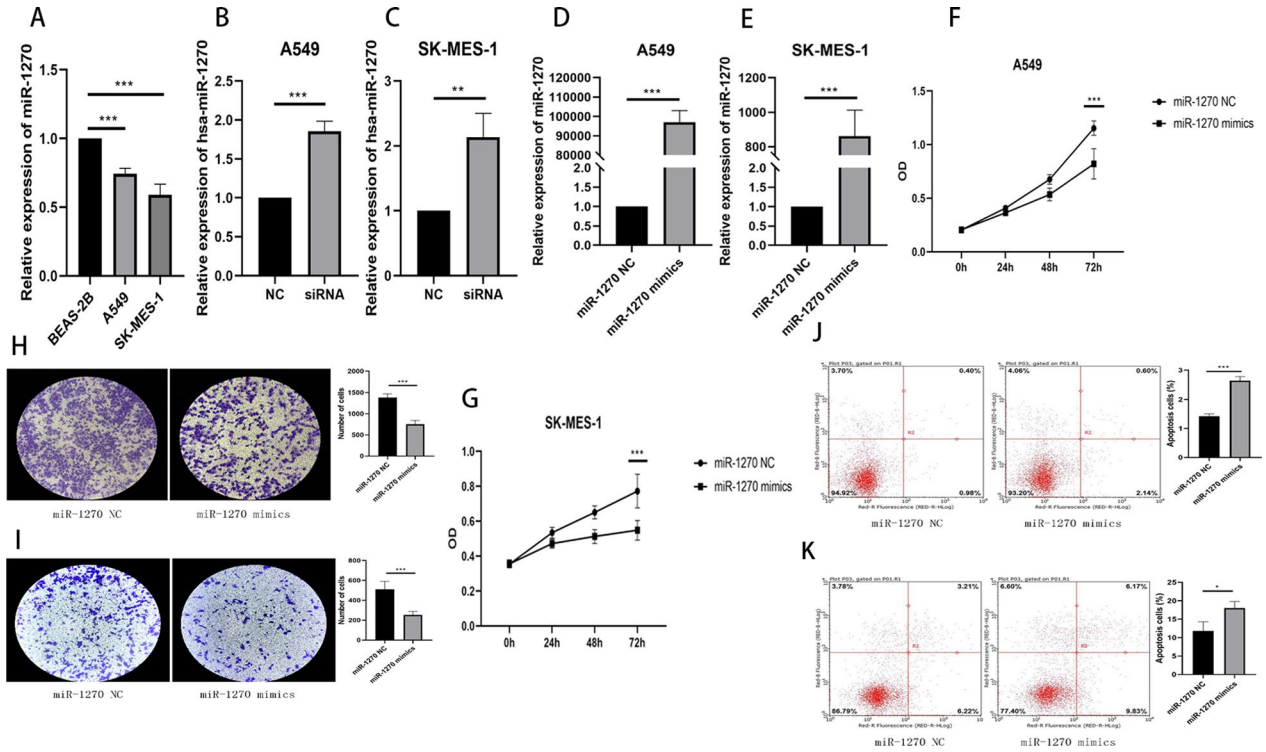

Fig. 4 **A** Expression of miR-1270 in BEAS-2B cells, A549 cells and SK-MES-1 cells; **B** the expression of miR-1270 was increased after circ_0072088 knockdown in A549 cells; **C** The expression of miR-1270 was increased after circ_0072088 knockdown in SK-MES-1 cells; **D** Expression of miR-1270 in A549 cells after transfection of NC and mimics; **E** Expression of miR-1270 in SK-MES-1 cells after transfection of NC and mimics; **F** Overexpression of miR-1270 inhibited cell proliferation in A549 cells; **G** Overexpression of miR-1270 inhibited cell proliferation in SK-MES-1 cells; **H** Overexpression of miR-1270 inhibited cell migration in A549 cells; **I** Overexpression of miR-1270 inhibited cell migration in SK-MES-1 cells; **J** Overexpression of miR-1270 promoted apoptosis of A549 cells; **K** Overexpression of miR-1270 promoted apoptosis of SK-MES-1 cells

the inhibitory effect of overexpression circ_0072088 on apoptosis was recovered due to the overexpression of miR-1270 ($P < 0.05$).

Effects of miR-1270 and circ_0072088 on TOP2A gene expression

The effect of overexpression of miR-1270 on TOP2A gene expression was investigated by qRT-PCR. As shown in Fig. 6A, B, compared with miR-1270 NC, the expression of TOP2A gene decreased after the overexpression of miR-1270, and the difference was statistically significant (A549, $P < 0.001$; SK-MES-1, $P < 0.001$).

Dual luciferase experiment was detected for targeted binding relationship

The targeted binding relationship between circ_0072088 and miR-1270.

As shown in Fig. 6C, the fluorescence intensity of the circ_0072088 WT + miR-1270 mimics group decreased in A549 cells and SK-MES-1 cells compared with that of the circ_0072088 WT + miR-1270 NC group (A549, $P < 0.01$; SK-MES-1, $P < 0.05$), but there was no significant difference in fluorescence intensity between circ_0072088 MUT + miR-1270 NC group and circ_0072088 MUT + miR-1270 mimics group.

The targeted binding relationship between miR-1270 and TOP2A.

As shown in Fig. 6D. In A549 and SK-MES-1 cells, the fluorescence intensity of co-transfected TOP2A WT + miR-1270 NC group was higher than that of co-transfected TOP2A WT + miR-1270 mimics group (A549, $P < 0.01$; SK-MES-1, $P < 0.001$), while there was no significant difference in fluorescence intensity between the TOP2A MUT + miR-1270 NC group and the TOP2A MUT + miR-1270 mimics group.

Discussion

As a global health problem, the symptoms of early lung cancer patients are not particularly obvious, so most lung cancer patients have been diagnosed at the advanced stage, thus delaying the best period of treatment. Therefore, early diagnosis of lung cancer is of utmost importance. By identifying sensitive and specific biomarkers, effective early detection can be achieved, which plays an

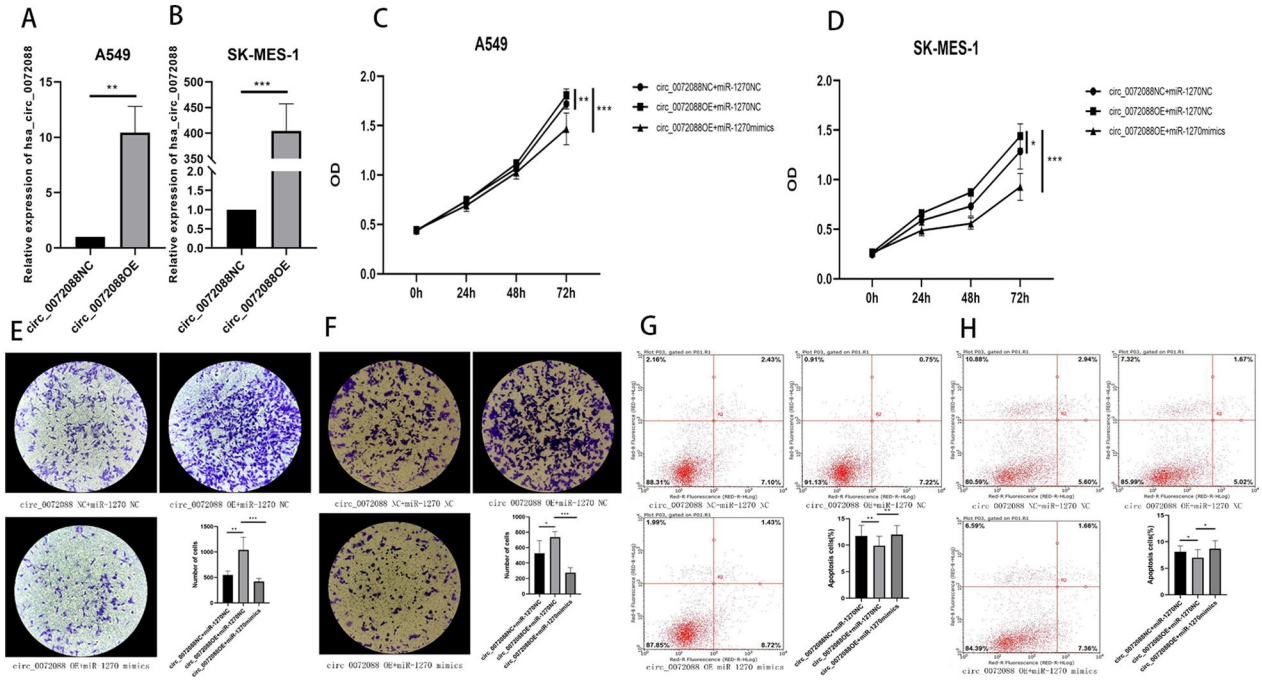

Fig. 5 **A** Expression of circ_0072088 in A549 cells after transfection with overexpressed plasmids; **B** Expression of circ_0072088 in SK-MES-1 cells after transfection with overexpressed plasmids; **C** circ_0072088 affects the proliferation ability of A549 cells by regulating miR-1270; **D** circ_0072088 affects the proliferation ability of SK-MES-1 cells by regulating miR-1270; **E** circ_0072088 affects cell migration ability of A549 cells by regulating miR-1270; **F** circ_0072088 affects cell migration ability of SK-MES-1 cells by regulating miR-1270; **G** circ_0072088 affects apoptosis of A549 cells regulating miR-1270; **H** circ_0072088 affects apoptosis of SK-MES-1 cells by regulating miR-1270

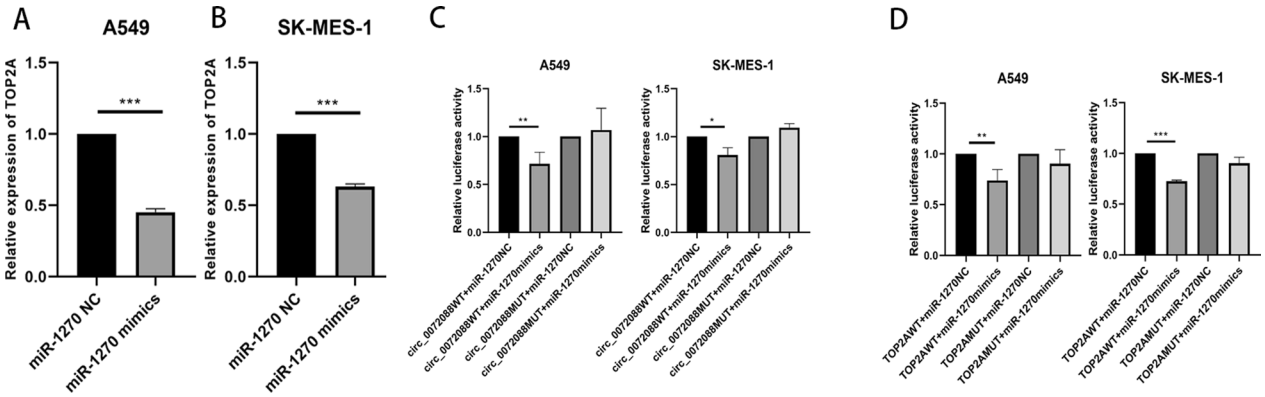

Fig. 6 **A** Expression of TOP2A gene decreased after the miR-1270 overexpression in A549 cells; **B** Expression of TOP2A gene decreased after the miR-1270 overexpression in SK-MES-1 cells; **C** The targeting binding relationship between circ_0072088 and miR-1270; **D** The targeting binding relationship between miR-1270 and TOP2A

important role in the treatment of lung cancer patients [22–26]. This study centered on exploring the role of circular RNA (circRNA) in lung cancer.

Firstly, studies related to circRNA expression in lung cancer tissues were searched in GEO database, and bioinformatic analysis was used to explore the differentially expressed circRNAs in lung cancer tissues. In this study, the 'limma' package of R software was used to analyze the differential expression of circRNAs in non-small cell lung cancer tissues, and 5 differentially expressed circRNAs were obtained. Among them, hsa_circRNA_103809 is differentially highly expressed in lung cancer tissues, while hsa_circRNA_102442, hsa_circRNA_102046, hsa_circRNA_103415 and hsa_circRNA_103820 are

differentially lowly expressed in lung cancer tissues. Study has found that the expression of hsa_circRNA_103809 (circ_0072088) is up-regulated in tumor tissues of non-small cell lung cancer through the analysis of GSE101586 data set and circRNA expression experiment in tissue samples. They found that hsa_circRNA_103809 influences the progression of non-small cell lung cancer by modulating the miR-377-5p/NOVA2 axis [27]. Liu et al. found that hsa_circRNA_103809 can promote the expression of ZNF121 gene through targeted binding with miR-4302. This, in turn, increases the level of the MYC protein in lung cancer cells and affects the progression of lung cancer [28]. Chi et al. found that the overexpression of hsa_circ_103820 has a significant inhibitory effect on the proliferation, migration and invasion of lung cancer cells. Their study found that hsa_circ_103820 can target miR-200b-3p, subsequently affecting the expression of LATS2 gene and SOCS6 gene and influencing the development of lung cancer [29]. Zhou et al. found that the expression of hsa_circ_0072309 in the serum of lung cancer patients was significantly down-regulated. Moreover, it was closely related to the pathological stage, lymph node metastasis and prognosis of these patients [30]. Tian et al. found that hsa_circRNA_102046 (hsa_circ_0043256) can affect cinnamaldehyde induced apoptosis in non-small cell lung cancer [31].

In this study, weighted gene co-expression network analysis (WGCNA) was further applied to explore differentially expressed circRNAs in GEO databases. Through research and analysis, it was found that darkturquoise module and darkorange module were correlated with non-small cell lung cancer. The key genes in the modules were investigated by analyzing Gene Significance (GS) and Module Membership (MM). A total of 12 circRNAs associated with non-small cell lung cancer were identified, among them 5 circRNAs were identified in the darkturquoise module: hsa_circRNA_103243 (hsa_circ_0001238), hsa_circRNA_101367 (hsa_circ_0001998), hsa_circRNA_103123 (hsa_circ_0002360), hsa_circRNA_102854 (hsa_circ_0057104) and hsa_circRNA_103511 (hsa_circ_0067971). Meanwhile, seven circRNAs were obtained in the darkorange module: hsa_circRNA_104499 (hsa_circ_0082564), hsa_circRNA_103948 (hsa_circ_0003528), hsa_circRNA_101777 (hsa_circ_0038718), hsa_circRNA_101873 (hsa_circ_0004315), hsa_circRNA_102898 (hsa_circ_0005307), hsa_circRNA_103809 (hsa_circ_0072088) and hsa_circRNA_101287 (hsa_circ_0008274). Zhang et al. found that hsa_circ_0002360 was differentially highly expressed in NSCLC tissues, and the overexpression of hsa_circ_0002360 promoted the proliferation, migration and invasion of NSCLC cells. Moreover, it can affect the expression of MMP16 by interacting with multiple microRNAs, and thus affect the progression of non-small cell lung cancer [32]. By intersecting the results of the 'limma' package difference analysis and the weighted gene co-expression network analysis (WGCNA), hsa_circRNA_103809 (hsa_circ_0072088) was obtained. This study will focus on hsa_circRNA_103809 (hsa_circ_0072088) to explore its association with non—small cell lung cancer.

In this study, circ_0072088 was found to be differentially highly expressed in lung adenocarcinoma A549 cells and lung squamous cell carcinoma SK-MES-1 cells when compared to normal lung epithelial cells. Moreover, it was found that the knockdown of circ_0072088 could affect the proliferation, migration and apoptosis of lung adenocarcinoma A549 cells and lung squamous cell carcinoma SK-MES-1 cells. Specifically, after circ_0072088 knockdown, the proliferation and migration of A549 and SK—MES—1 cells were inhibited, while cell apoptosis was promoted. Similarly, Cao et al. found that the circ_0072088 expression was up-regulated in lung adenocarcinoma tissues compared to adjacent normal tissues. They also found that the proliferation, migration and invasion of H1299 cells were inhibited after circ_0072088 knockdown [33]. In studies related to cervical cancer, Zhou et al. found that knocking down circ_0072088 inhibited the proliferation, migration and invasion of cervical cancer cells. After circ_0072088 knockdown, the number of cells in the G0-G1 phase increased, while the number of cells in the S phase decreased [34]. Therefore, due to its important role in cancer, circ_0072088 may serve as a potential biomarker of cancer and provide clues for molecular level research on cancer.

Hsa_circ_0072088 (circZFR, hsa_circRNA_103809) plays an important role in cancer [35]. Multiple studies have found that hsa_circ_0072088 plays a potential role in the proliferation, migration, invasion, and apoptosis of various tumor cells. Consequently, it is believed that hsa_circ_0072088 can influence the progression of cancer [36–38]. Among the numerous potential mechanisms related to hsa_circ_0072088, the most extensively studied is its competing endogenous RNA (ceRNA) mechanism. That is, hsa_circ_0072088 regulates the target genes downstream of microRNA by targeting and binding to microRNA. For example, there is a targeted binding between hsa_circ_0072088 and miR—377. The study by Zhang et al. found that the hsa_circ_0072088/miR—377/ZEB2 axis plays an important role in bladder cancer [39]. Fang et al.'s research revealed the significant role of the hsa_circ_0072088/miR—377/VEGF axis in esophageal squamous cell carcinoma [37]. In research related to non—small cell lung cancer, Zhang et al. discovered that the circ_0072088/miR—944/LASP1 axis influences the progression of non—small cell lung cancer

[40]. In hepatocellular carcinoma related research, the study by Li et al. found that circ_0072088 is differentially highly expressed in hepatocellular carcinoma. Moreover, circ_0072088 regulates the proliferation, migration, invasion, and apoptosis of hepatocellular carcinoma cells. circ_0072088 binds to miR—375 in a targeted manner, thereby regulating the expression of its downstream gene JAK2, and thus regulating the JAK2/STAT3 signaling pathway [38]. In research related to thyroid cancer, Xiong et al. expounded that hsa_circ_0072088 can act as a "sponge" for miR—16, thereby regulating the expression of its downstream target gene MAPK1, and consequently regulating the progression of thyroid cancer [41]. This study is also committed to exploring the ceRNA mechanism of hsa_circ_0072088 in non—small cell lung cancer.

This study found that miR-1270 was differentially lowly expressed in A549 cells and SK-MES-1 cells. Overexpression of miR-1270 inhibited cell proliferation and migration, while promoting cell apoptosis. The ceRNA mechanism is a crucial way through which miR—1270 exerts its effects in cancer. In studies related to liver cancer, Sun et al. found that circ_0088364 regulates the growth and movement of liver cancer cells through the circ_0088364/miR-1270/COL4A1 axis [42]. In cervical cancer, Wang et al. found that circ_0001247 acts as a 'sponge' of miR-1270, regulating the progression of cervical cancer by up-regulating the expression level of ZEB2 [43]. The study of Gao et al. found that circ-SOX4 regulates the expression of PLAGL2 by acting as a 'sponge' of miR-1270, thereby affecting the WNT signal pathway and regulating the occurrence and development of lung adenocarcinoma [44]. According to the study of Zhao et al., circular RNA Cdr1as affects the expression of SCAI by binding to miR-1270, thus affecting cisplatin resistance in ovarian cancer [45]. In bladder cancer, it has been found that circular RNA Cdr1as acts as a 'sponge' of miR-1270 to regulate the expression of APAF1, thereby affecting the sensitivity of bladder cancer to cisplatin [46]. In conclusion, miR-1270 can regulate cancer development and drug sensitivity in tumor therapy by binding to multiple circRNAs. In this study, it was found that circ_0072088 could interact with miR-1270 through targeted binding, and this interaction was verified by the rescue experiment and dual luciferase experiment. In this study, it was found that cell proliferation and cell migration of A549 cells and SK-MES-1 cells were promoted after the overexpression of circ_0072088. Further overexpression of miR-1270 on the basis of circ_0072088 overexpression can inhibit the promotion of cell proliferation and cell migration caused by circ_0072088 overexpression. Similarly, the apoptosis of A549 cells and SK-MES-1 cells was inhibited after circ_0072088 overexpression. Further overexpression of miR-1270 on the basis of overexpression of circ_0072088 can restore the inhibitory effect of overexpression of circ_0072088 on apoptosis. The interaction between circ_0072088 and miR—1270 has also been verified in hepatocellular carcinoma and bladder cancer. In hepatocellular carcinoma, it has been found that circ-0072088 (hsa-circRNA-103809) regulates the development of liver cancer by influencing the expression of PLAGL2 through interaction with miR-1270 [47]. In bladder cancer, circ-ZFR regulates the expression of WNT5A by acting as a 'sponge' for miR-545 and miR-1270, thereby regulating the progression of bladder cancer [48].

Topoisomerase II (TOPO II) plays an important role in cell division. Vertebrates encode two TOP2 subtypes, TOP2A and TOP2B [49]. Among them TOP2A is essential for cell division [50, 51]. TOP2A expression has been found to be associated with patient prognosis in a variety of tumor-related studies [52–54]. In the research exploring the interaction between TOP2A and microRNA, Zhang et al. found that miR-599 can affect the progression of bladder cancer by regulating its target gene TOP2A [55]. Study has shown that TOP2A plays an important role in the progression of liver cancer. TOP2A affects the EMT of liver cancer cells through Hippo signaling pathway, thereby promoting the invasion and migration of liver cancer cells. Additionally, it can interact with miR-22-5p, which suggests that TOP2A may serve as a prognostic biomarker and therapeutic target for liver cancer [56]. Study has found that TOP2A may be associated with the prognosis of triple-negative breast cancer [57]. Therefore, TOP2A may be a potential biomarker and therapeutic target for cancer.

Conclusion

In this study, through bioinformatics analysis, we identified hsa_circRNA_103809 (hsa_circ_0072088) as the circRNA of interest and further identified its potential ceRNA mechanism: hsa_circ_0072088/miR-1270/TOP2A. In this study, we found that circ_0072088 was differentially highly expressed in lung adenocarcinoma A549 cells and lung squamous cell carcinoma SK-MES-1 cells. Silencing circ_0072088 could inhibit the proliferation and migration of non-small cell lung cancer cells while promote cell apoptosis. The expression of miR-1270 was differentially low in A549 cells and SK-MES-1 cells, and overexpression of miR-1270 also inhibited cell proliferation and cell migration of NSCLC cells and promoted cell apoptosis. In addition, this study revealed that circ_0072088 can regulate the expression of TOP2A by acting as a 'sponge' of miR-1270, thereby regulating the progression of NSCLC. In conclusion, circ_0072088 may serve as a potential biomarker for non-small cell lung cancer.

Supplementary Information

The online version contains supplementary material available at https://doi.org/10.1186/s12935-025-03749-3.

Additional file 1.

Additional file 2.

Additional file 3.

Additional file 4.

Author contributions

Sixuan Li makes significant contributions in data acquisition, data analysis and is responsible for drafting this article. Zhigang Cui, Min Gao and Yanan Shan play a major role in design ideas, data acquisition and was responsible for grammar and spelling checks. Yihong Ren, Yuxin Zhao, Di Wang and Tingyu Meng make significant contributions to data acquisition and analysis. Hongxu Liu was primarily responsible for providing constructive suggestions for the revision of the manuscript and carefully refining and perfecting its structure, content, and language expression. Zhihua Yin is responsible for the correction of the article and the final approval of the publication version.

Funding

This work was supported by Project of Natural Science Foundation of Liaoning Province (2023-MSLH-368).

Data availability

The data generated in this study are publicly available in TCGA database and GEO database at https://portal.gdc.cancer.gov/ and https://www.ncbi.nlm.nih.gov/geo/.

Declarations

Ethics approval and consent to participate

All study participants provided informed consent, and the study design was approved by ethics review board.

Competing interests

The authors have no relevant financial or non-financial interests to disclose.

Author details

[1]Postdoctoral Research Station, Cancer Hospital of Dalian University of Technology, Liaoning Cancer Hospital & Institute, Shenyang 110042, China. [2]Department of Epidemiology, School of Public Health, China Medical University, Shenyang 110122, Liaoning, China. [3]Department of Thoracic Surgery, Cancer Hospital of Dalian University of Technology, Liaoning Cancer Hospital & Institute, Shenyang 110042, China. [4]School of Nursing, China Medical University, Shenyang 110122, Liaoning, China.

Received: 10 May 2024 Accepted: 12 March 2025
Published online: 21 April 2025

References

1. Sung H, Ferlay J, Siegel RL, Laversanne M, Soerjomataram I, Jemal A, Bray F. Global cancer statistics 2020: GLOBOCAN estimates of incidence and mortality worldwide for 36 cancers in 185 countries. CA: Cancer J Clin. 2021;71(3):209–49. https://doi.org/10.3322/caac.21660.
2. Cao W, Chen HD, Yu YW, Li N, Chen WQ. Changing profiles of cancer burden worldwide and in China: a secondary analysis of the global cancer statistics 2020. Chin Med J. 2021;134:783–91. https://doi.org/10.1097/cm9.0000000000001474.
3. Lasda E, Parker R. Circular RNAs: diversity of form and function. RNA (New York, NY). 2014;20:1829–42. https://doi.org/10.1261/rna.047126.114.
4. Sanger HL, Klotz G, Riesner D, Gross HJ, Kleinschmidt AK. Viroids are single-stranded covalently closed circular RNA molecules existing as highly base-paired rod-like structures. Proc Natl Acad Sci USA. 1976;73:3852–6. https://doi.org/10.1073/pnas.73.11.3852.
5. Hsu MT, Coca-Prados M. Electron microscopic evidence for the circular form of RNA in the cytoplasm of eukaryotic cells. Nature. 1979;280:339–40. https://doi.org/10.1038/280339a0.
6. Nigro JM, Cho KR, Fearon ER, Kern SE, Ruppert JM, Oliner JD, Kinzler KW, Vogelstein B. Scrambled exons. Cell. 1991;64:607–13. https://doi.org/10.1016/0092-8674(91)90244-s.
7. Cocquerelle C, Mascrez B, Hétuin D, Bailleul B. Mis-splicing yields circular RNA molecules. FASEB J : Off Publ Fed Am Soc Exp Biol. 1993;7:155–60. https://doi.org/10.1096/fasebj.7.1.7678559.
8. Capel B, Swain A, Nicolis S, Hacker A, Walter M, Koopman P, Goodfellow P, Lovell-Badge R. Circular transcripts of the testis-determining gene Sry in adult mouse testis. Cell. 1993;73:1019–30. https://doi.org/10.1016/0092-8674(93)90279-y.
9. Xiao MS, Ai Y, Wilusz JE. Biogenesis and functions of circular RNAs come into focus. Trends Cell Biol. 2020;30:226–40. https://doi.org/10.1016/j.tcb.2019.12.004.
10. Salmena L, Poliseno L, Tay Y, Kats L, Pandolfi PP. A ceRNA hypothesis: the Rosetta Stone of a hidden RNA language? Cell. 2011. https://doi.org/10.1016/j.cell.2011.07.014.
11. Tay Y, Rinn J, Pandolfi PP. The multilayered complexity of ceRNA crosstalk and competition. Nature. 2014;505(7483):344–52. https://doi.org/10.1038/nature12986.
12. Zhang X, Wang S, Wang H, Cao J, Huang X, Chen Z, Xu P, Sun G, Xu J, Lv J, Xu Z. Circular RNA circNRIP1 acts as a microRNA-149-5p sponge to promote gastric cancer progression via the AKT1/mTOR pathway. Mol Cancer. 2019;18:20. https://doi.org/10.1186/s12943-018-0935-5.
13. Luo Z, Rong Z, Zhang J, Zhu Z, Yu Z, Li T, Fu Z, Qiu Z, Huang C. Circular RNA circCCDC9 acts as a miR-6792-3p sponge to suppress the progression of gastric cancer through regulating CAV1 expression. Mol Cancer. 2020;19:86. https://doi.org/10.1186/s12943-020-01203-8.
14. Peng L, Sang H, Wei S, Li Y, Jin D, Zhu X, Li X, Dang Y, Zhang G. circCUL2 regulates gastric cancer malignant transformation and cisplatin resistance by modulating autophagy activation via miR-142-3p/ROCK2. Mol Cancer. 2020;19:156. https://doi.org/10.1186/s12943-020-01270-x.
15. Qi L, Sun B, Yang B, Lu S. CircMMP11 regulates proliferation, migration, invasion, and apoptosis of breast cancer cells through miR-625-5p/ZEB2 axis. Cancer Cell Int. 2021;21:133. https://doi.org/10.1186/s12935-021-01816-z.
16. Xu JZ, Shao CC, Wang XJ, Zhao X, Chen JQ, Ouyang YX, Feng J, Zhang F, Huang WH, Ying Q, Chen CF, Wei XL, Dong HY, Zhang GJ, Chen M. circTADA2As suppress breast cancer progression and metastasis via targeting miR-203a-3p/SOCS3 axis. Cell Death Dis. 2019;10:175. https://doi.org/10.1038/s41419-019-1382-y.
17. Lu Q, Liu T, Feng H, Yang R, Zhao X, Chen W, Jiang B, Qin H, Guo X, Liu M, Li L, Guo H. Circular RNA circSLC8A1 acts as a sponge of miR-130b/miR-494 in suppressing bladder cancer progression via regulating PTEN. Mol Cancer. 2019;18:111. https://doi.org/10.1186/s12943-019-1040-0.
18. Zhang C, Liu P, Huang J, Liao Y, Pan C, Liu J, Du Q, Liu T, Shang C, Ooi S, Chen R, Xia M, Jiang H, Xu M, Zou Q, Zhou Y, Huang H, Pan Y, Yuan L, Wang W, Yao S. Circular RNA hsa_circ_0043280 inhibits cervical cancer tumor growth and metastasis via miR-203a-3p/PAQR3 axis. Cell Death Dis. 2021;12:888. https://doi.org/10.1038/s41419-021-04193-7.
19. Chen S, Hong K, Zhou L, Ran R, Huang J, Zheng Y, Xing M, Cai Y. Hsa_circRNA_0017620 regulated cell progression of non-small-cell lung cancer via miR-520a-5p/KRT5 axis. J Clin Lab Anal. 2022;36:e24347. https://doi.org/10.1002/jcla.24347.
20. Ma X, Yang X, Bao W, Li S, Liang S, Sun Y, Zhao Y, Wang J, Zhao C. Circular RNA circMAN2B2 facilitates lung cancer cell proliferation and invasion via miR-1275/FOXK1 axis. Biochem Biophys Res Commun. 2018;498:1009–15. https://doi.org/10.1016/j.bbrc.2018.03.105.
21. Man W, Cui Y, Li J, Li Y, Jin J, Jin Y, Wu X, Zhong R, Li X, Yao H, Lin Y, Jiang L, Wang Y. circTAB2 inhibits lung cancer proliferation, migration and invasion by sponging miR-3142 to upregulate GLIS2. Apoptosis : Int J Program Cell Death. 2023;28:471–84. https://doi.org/10.1007/s10495-022-01805-1.
22. Chu GCW, Lazare K, Sullivan F. Serum and blood based biomarkers for lung cancer screening: a systematic review. BMC Cancer. 2018;18:181. https://doi.org/10.1186/s12885-018-4024-3.
23. Nooreldeen R, Bach H. Current and future development in lung cancer diagnosis. Int J Mol Sci. 2021. https://doi.org/10.3390/ijms22168661.

24. Seijo LM, Peled N, Ajona D, Boeri M, Field JK, Sozzi G, Pio R, Zulueta JJ, Spira A, Massion PP, Mazzone PJ, Montuenga LM. Biomarkers in lung cancer screening: achievements, promises, and challenges. J Thorac Oncol : Off Publ Int Assoc Study Lung Cancer. 2019;14:343–57. https://doi.org/10.1016/j.jtho.2018.11.023.
25. Villalobos P, Wistuba II. Lung cancer biomarkers. Hematol Oncol Clin North Am. 2017;31:13–29. https://doi.org/10.1016/j.hoc.2016.08.006.
26. Zito Marino F, Bianco R, Accardo M, Ronchi A, Cozzolino I, Morgillo F, Rossi G, Franco R. Molecular heterogeneity in lung cancer: from mechanisms of origin to clinical implications. Int J Med Sci. 2019;16:981–9. https://doi.org/10.7150/ijms.34739.
27. Tan Z, Cao F, Jia B, Xia L. Circ_0072088 promotes the development of non-small cell lung cancer via the miR-377-5p/NOVA2 axis. Thorac cancer. 2020;11:2224–36. https://doi.org/10.1111/1759-7714.13529.
28. Liu W, Ma W, Yuan Y, Zhang Y, Sun S. Circular RNA hsa_circRNA_103809 promotes lung cancer progression via facilitating ZNF121-dependent MYC expression by sequestering miR-4302. Biochem Biophys Res Commun. 2018;500:846–51. https://doi.org/10.1016/j.bbrc.2018.04.172.
29. Chi Y, Zheng W, Bao G, Wu L, He X, Gan R, Shen Y, Yin X, Jin M. Circular RNA circ_103820 suppresses lung cancer tumorigenesis by sponging miR-200b-3p to release LATS2 and SOCS6. Cell Death Dis. 2021;12:185. https://doi.org/10.1038/s41419-021-03472-7.
30. Zhou Y, Tong Z, Zhu X, Huang S, Dong Z, Ye Z. hsa_circ_0072309 expression profiling in non-small-cell lung carcinoma and its implications for diagnosis and prognosis. Front Surg. 2022;9:842292. https://doi.org/10.3389/fsurg.2022.842292.
31. Tian F, Yu CT, Ye WD, Wang Q. Cinnamaldehyde induces cell apoptosis mediated by a novel circular RNA hsa_circ_0043256 in non-small cell lung cancer. Biochem Biophys Res Commun. 2017;493:1260–6. https://doi.org/10.1016/j.bbrc.2017.09.136.
32. Zhang Y, Zeng S, Wang T. Circular RNA hsa_circ_0002360 promotes non-small cell lung cancer progression through upregulating matrix metalloproteinase 16 and sponging multiple micorRNAs. Bioengineered. 2021;12:12767–77. https://doi.org/10.1080/21655979.2021.1999370.
33. Cao F, Liu S, Li Z, Meng L, Sang M, Shan B. Activation of circ_0072088/miR-1261/PIK3CA pathway accelerates lung adenocarcinoma progression. Thorac Cancer. 2022;13:1548–57. https://doi.org/10.1111/1759-7714.14369.
34. Zhou M, Yang Z, Wang D, Chen P, Zhang Y. The circular RNA circZFR phosphorylates Rb promoting cervical cancer progression by regulating the SSBP1/CDK2/cyclin E1 complex. J Exp Clin Cancer Res: CR. 2021;40:48. https://doi.org/10.1186/s13046-021-01849-2.
35. Liu L, Wang H, Yu S, Gao X, Liu G, Sun D, Jiang X. An update on the roles of circRNA-ZFR in human malignant tumors. Front Cell Dev Biol. 2021;9:806181. https://doi.org/10.3389/fcell.2021.806181.
36. Bian L, Zhi X, Ma L, Zhang J, Chen P, Sun S, Li J, Sun Y, Qin J. Hsa_circRNA_103809 regulated the cell proliferation and migration in colorectal cancer via miR-532-3p / FOXO4 axis. Biochem Biophys Res Commun. 2018;505:346–52. https://doi.org/10.1016/j.bbrc.2018.09.073.
37. Fang N, Shi Y, Fan Y, Long T, Shu Y, Zhou J. Circ_0072088 Promotes proliferation, migration, and invasion of Esophageal squamous cell cancer by absorbing miR-377. J Oncol. 2020;2020:8967126. https://doi.org/10.1155/2020/8967126.
38. Li L, Xiao C, He K, Xiang G. Circ_0072088 promotes progression of hepatocellular carcinoma by activating JAK2/STAT3 signaling pathway via miR-375. IUBMB Life. 2021;73:1153–65. https://doi.org/10.1002/iub.2520.
39. Zhang WY, Liu QH, Wang TJ, Zhao J, Cheng XH, Wang JS. CircZFR serves as a prognostic marker to promote bladder cancer progression by regulating miR-377/ZEB2 signaling. 2019. Biosci Rep. https://doi.org/10.1042/bsr20192779.
40. Zhang L, Wu Y, Hou C, Li F. Circ_0072088 knockdown contributes to cisplatin sensitivity and inhibits tumor progression by miR-944/LASP1 axis in non-small cell lung cancer. J Gene Med. 2022;24:e3414. https://doi.org/10.1002/jgm.3414.
41. Xiong H, Yu H, Jia G, Yu J, Su Y, Zhang J, Zhou J. circZFR regulates thyroid cancer progression by the miR-16/MAPK1 axis. Environ Toxicol. 2021;36:2236–44. https://doi.org/10.1002/tox.23337.
42. Sun K, Wang H, Zhang D, Li Y, Ren L. Depleting circ_0088364 restrained cell growth and motility of human hepatocellular carcinoma via circ_0088364-miR-1270-COL4A1 ceRNA pathway. Cell Cycle (Georgetown, Tex). 2022;21:261–75. https://doi.org/10.1080/15384101.2021.2016196.
43. Wang W, Xu A, Zhao M, Sun J, Gao L. Circ_0001247 functions as a miR-1270 sponge to accelerate cervical cancer progression by up-regulating ZEB2 expression level. Biotech Lett. 2021;43:745–55. https://doi.org/10.1007/s10529-020-03059-w.
44. Gao N, Ye B. Circ-SOX4 drives the tumorigenesis and development of lung adenocarcinoma via sponging miR-1270 and modulating PLAGL2 to activate WNT signaling pathway. Cancer Cell Int. 2020;20:2. https://doi.org/10.1186/s12935-019-1065-x.
45. Zhao Z, Ji M, Wang Q, He N, Li Y. Circular RNA Cdr1as upregulates SCAI to suppress Cisplatin resistance in Ovarian cancer via miR-1270 Suppression. Mol Ther Nucl Acids. 2019;18:24–33. https://doi.org/10.1016/j.omtn.2019.07.012.
46. Yuan W, Zhou R, Wang J, Han J, Yang X, Yu H, Lu H, Zhang X, Li P, Tao J, Wei J, Lu Q, Yang H, Gu M. Circular RNA Cdr1as sensitizes bladder cancer to cisplatin by upregulating APAF1 expression through miR-1270 inhibition. Mol Oncol. 2019;13:1559–76. https://doi.org/10.1002/1878-0261.12523.
47. Cao Y, Tao Q, Kao X, Zhu X. Hsa-circRNA-103809 promotes hepatocellular carcinoma development via MicroRNA-1270/PLAG1 like zinc finger 2 axis. Dig Dis Sci. 2021;66:1524–32. https://doi.org/10.1007/s10620-020-06416-x.
48. Luo L, Miao P, Ming Y, Tao J, Shen H. Circ-ZFR promotes progression of bladder cancer by upregulating WNT5A via sponging miR-545 and miR-1270. Front Oncol. 2020;10:596623. https://doi.org/10.3389/fonc.2020.596623.
49. Uusküla-Reimand L, Wilson MD. Untangling the roles of TOP2A and TOP2B in transcription and cancer. Sci Adv. 2022;8(44):eadd4920. https://doi.org/10.1126/sciadv.add4920.
50. Grue P, Grässer A, Sehested M, Jensen PB, Uhse A, Straub T, Ness W, Boege F. Essential mitotic functions of DNA topoisomerase IIalpha are not adopted by topoisomerase IIbeta in human H69 cells. J Biol Chem. 1998;273:33660–6. https://doi.org/10.1074/jbc.273.50.33660.
51. Lee JH, Berger JM. Cell cycle-dependent control and roles of DNA Topoisomerase II. Genes. 2019. https://doi.org/10.3390/genes10110859.
52. An X, Xu F, Luo R, Zheng Q, Lu J, Yang Y, Qin T, Yuan Z, Shi Y, Jiang W, Wang S. The prognostic significance of topoisomerase II alpha protein in early stage luminal breast cancer. BMC Cancer. 2018;18:331. https://doi.org/10.1186/s12885-018-4170-7.
53. Gao XH, Yu ZQ, Zhang C, Bai CG, Zheng JM, Fu CG. DNA topoisomerase II alpha: a favorable prognostic factor in colorectal caner. Int J Colorectal Dis. 2012;27:429–35. https://doi.org/10.1007/s00384-011-1346-x.
54. Wu Y, Han Y, Li Q, Zhang P, Yuan P, Luo Y, Fan Y, Chen S, Cai R, Li Q, Xu H, Wang Y, Ma F, Wang J, Xu B. Predictive value of topoisomerase II alpha protein for clinicopathological characteristics and prognosis in early breast cancer. Breast Cancer Res Treat. 2022;193:381–92. https://doi.org/10.1007/s10549-022-06559-7.
55. Zhang F, Wu H. MiR-599 targeting TOP2A inhibits the malignancy of bladder cancer cells. Biochem Biophys Res Commun. 2021;570:154–61. https://doi.org/10.1016/j.bbrc.2021.06.069.
56. Zhao H, Chen C, Song H, Qin R, Wang X, He Q, Li F, Zhao H, Li Y. DNA Topoisomerase II-α regulated by miR-22-5p promotes hepatocellular carcinoma invasion and migration through the hippo pathway. Oxid Med Cell Longev. 2022;2022:4277254. https://doi.org/10.1155/2022/4277254.
57. Ma J, Chen C, Liu S, Ji J, Wu D, Huang P, Wei D, Fan Z, Ren L. Identification of a five genes prognosis signature for triple-negative breast cancer using multi-omics methods and bioinformatics analysis. Cancer Gene Ther. 2022;29:1578–89. https://doi.org/10.1038/s41417-022-00473-2.

Publisher's Note